

Supporting Information for "Evaporative Resistance is of Equal Importance as Surface Albedo in High Latitude Surface Temperatures Due to Cloud Feedbacks"

Jinhyuk E. Kim¹, Marysa M. Laguë^{1,2}, Sam Pennypacker¹, Eliza Dawson^{1,3},

Abigail L.S. Swann^{1,4}

¹Department of Atmospheric Sciences, University of Washington, Seattle, WA 98195, USA

²Now at Department of Earth and Planetary Science, University of California Berkeley, Berkeley, CA 94709, USA

³Now at School of Earth, Energy, and Environmental Sciences, Stanford University, Stanford, CA 94305, USA

⁴Department of Biology, University of Washington, Seattle, WA 98195, USA

1. Further discussion of SLIM

1.1. Evaporative Resistance

In a complex land surface model, and in a real forest, multiple factors control how difficult it is for water to be evaporated or transpired from the land surface to the atmosphere, such as leaf-level stomatal conductance, leaf area, root depth, and soil moisture. In SLIM, the resistance to evaporation (which modulates the magnitude of the latent heat flux) is controlled by two individual resistance terms. The first term is a time varying function of how much water is being stored in the land surface analogous to soil mois-

ture, with a higher resistance at low moisture. The second term is user-prescribed and represents the bulk, canopy-level resistance to evaporation analogous to the vegetation-controlled processes and properties such as stomatal conductance and leaf area. For the purposes of this study, changes in “evaporative resistance” refer to changes in the second term. It should be noted that within SLIM, vegetation height, which is used to modulate large-scale turbulent exchange with the atmosphere, is independent of the canopy-level resistance. Details of the flux calculations in SLIM can be found in the SLIM model description (Laguë et al., 2019).

Our experimental setup is able to capture some, but not all feedbacks between the land and the atmosphere. The atmosphere is allowed to respond to the land surface, which is essential for calculating the effects of land surface changes on surface temperatures (Laguë et al., 2019). In particular, this allows for substantial changes in latent heat flux under different atmospheric conditions. However, the prescribed evaporative resistance can only be altered by a change in soil moisture, and is not altered by changes in relative humidity, wind speed, etc. of the overlying atmosphere.

2. Statistics

2.1. Autocorrelation and Degrees of Freedom

Based on previous analysis of autocorrelation in this model, we find this to be a conservative estimate of the degrees of freedom in our data, which we demonstrate in two ways. First, the autocorrelation of our data (in this case, global average temperature and Arctic average temperature) is small after two years (Fig. S3). Second, we follow the methodology of Bretherton, Widmann, Dymnikov, Wallace, and Bladé (1999) to estimate

the effective degrees of freedom, N^* , in serially correlated data with $N=15$ samples using the following equation:

$$N^* = N \frac{1 - r_x r_x}{1 + r_x r_x} \quad (1)$$

where r_x is the lag-1 autocorrelation of some variable x (eg 2m air temperature) with itself. This holds for $r_x \ll 1$, which is shown to be true in a large spatial average in Fig. S3. Applying this equation, we can calculate the effective degrees of freedom N^* spatially (Fig. S4), and find that the effective degrees of freedom is larger than 15 in almost all grid-cells, with a globally averaged effective degrees of freedom of 27.

References

- Bretherton, C. S., Widmann, M., Dymnikov, V. P., Wallace, J. M., & Bladé, I. (1999). The effective number of spatial degrees of freedom of a time-varying field. *Journal of Climate*. doi: 10.1175/1520-0442(1999)012<1990:TENOSD>2.0.CO;2
- Laguë, M. M. L., Bonan, G. B., & Swann, A. L. S. (2019). Separating the impact of individual land surface properties on the terrestrial surface energy budget in both the coupled and un-coupled land-atmosphere system. *Journal of Climate*.

Table S1: Albedo and evaporative resistance values for our vegetation types.

Surface Properties	Needleleaf	Broadleaf
Visible Direct	0.03	0.09
Visible Diffuse	0.04	0.10
Infrared Direct	0.14	0.18
Infrared Diffuse	0.17	0.20
Evaporative Resistance (s/m)	175	92

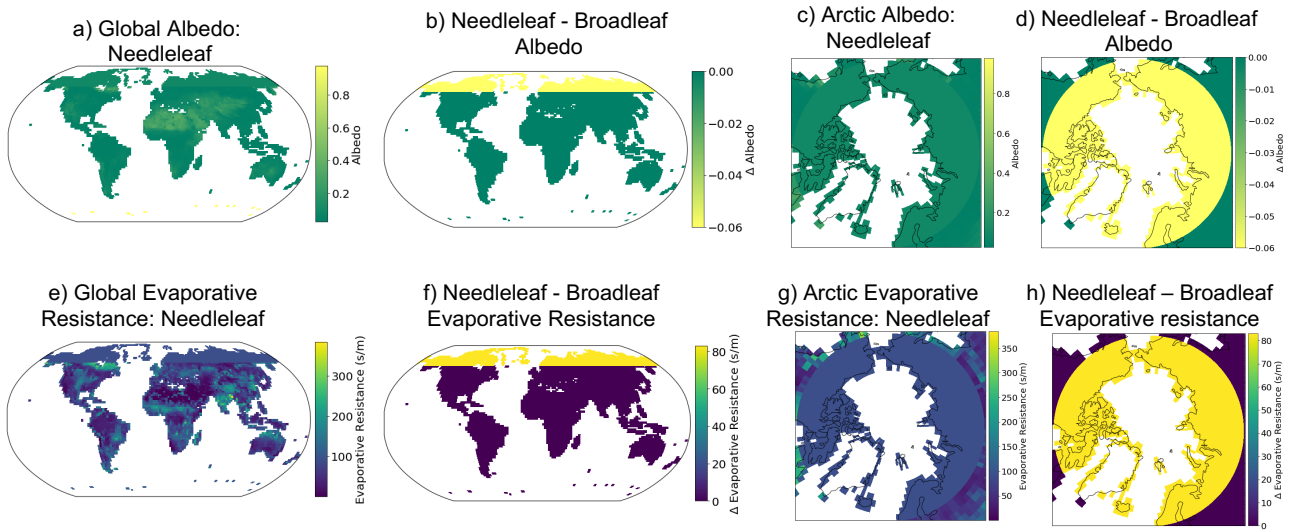


Figure S1: **Baseline Surface Properties for Broadleaf:** Our simulations are based on changes to albedo and evaporative resistance to the Arctic land surface (non-glaciated land North of 60N). When we change evaporative resistance and albedo we only change surface properties over non-glaciated land North of 60N which vary with the different simulations (Needleleaf, Bright Needleleaf, Dark Broadleaf, and Broadleaf. Panel a) shows the global baseline albedo of the surface of the Needleleaf simulation. Panel b) shows difference in albedo between the Needleleaf and Broadleaf simulation with the only changes between the simulation being in the Arctic. Panel c) is the Arctic map of albedo for the Needleleaf simulation and panel d) is the difference in albedo in the Arctic between the Needleleaf and Broadleaf simulation. Panel e) is the same as panel a) except showing evaporative resistance. Panel f) is the same as panel b) but for evaporative resistance. Panel g) is the same as panel c) but for evaporative resistance. Panel h) is the same as panel d) but for evaporative resistance.

Global Mean Temperatures

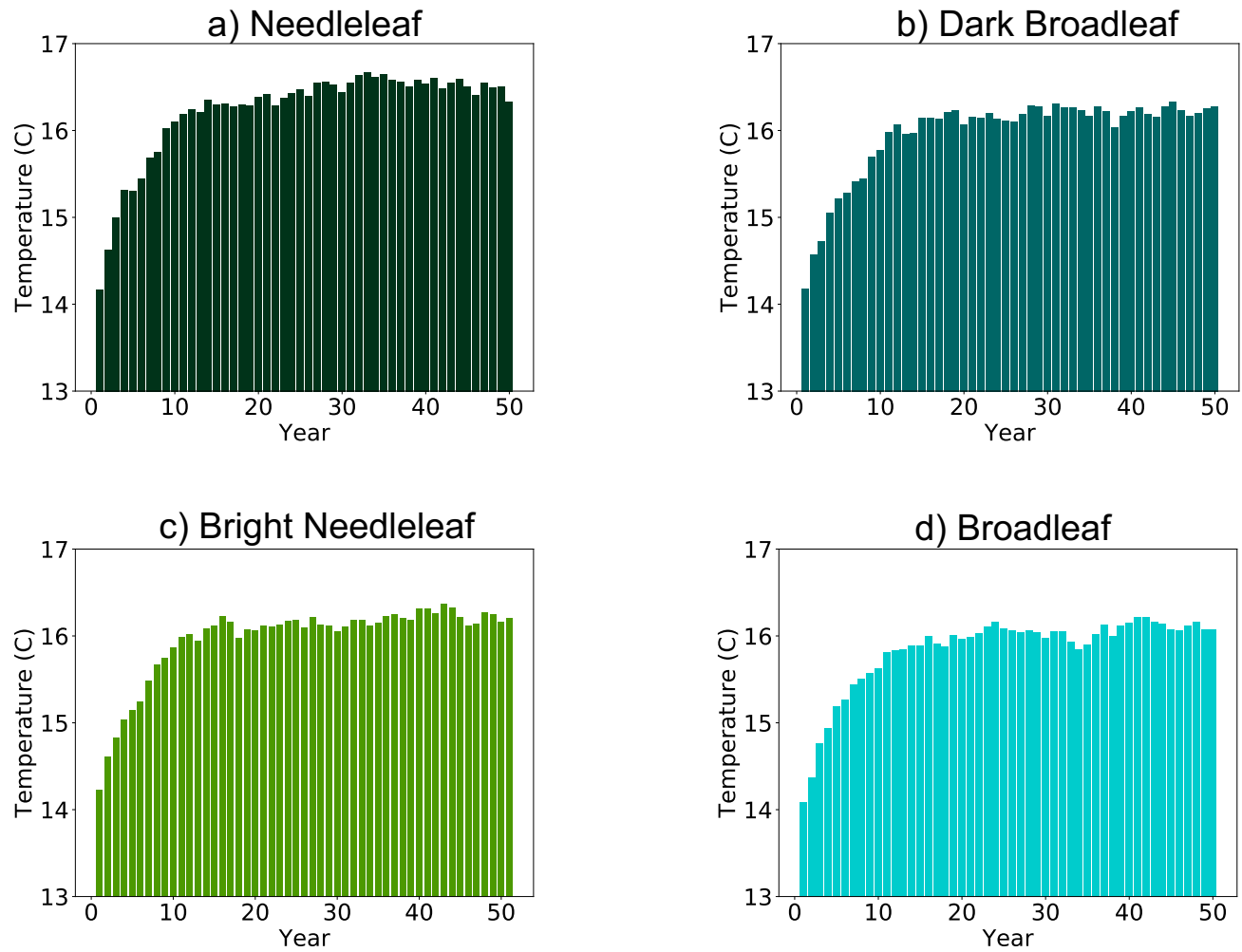


Figure S2: **Global mean 2m air temperatures.** Area-weighted averages for annual mean global 2m air temperatures each of four different simulations, a) Needleleaf, b) Dark Broadleaf, c) Bright Needleleaf, d) Broadleaf. Simulations have a negligible amount of drift in global mean 2m air temperatures for the last 30 years (less than $0.005^{\circ}\text{Cyear}^{-1}$), indicating that the simulations have reached equilibrium

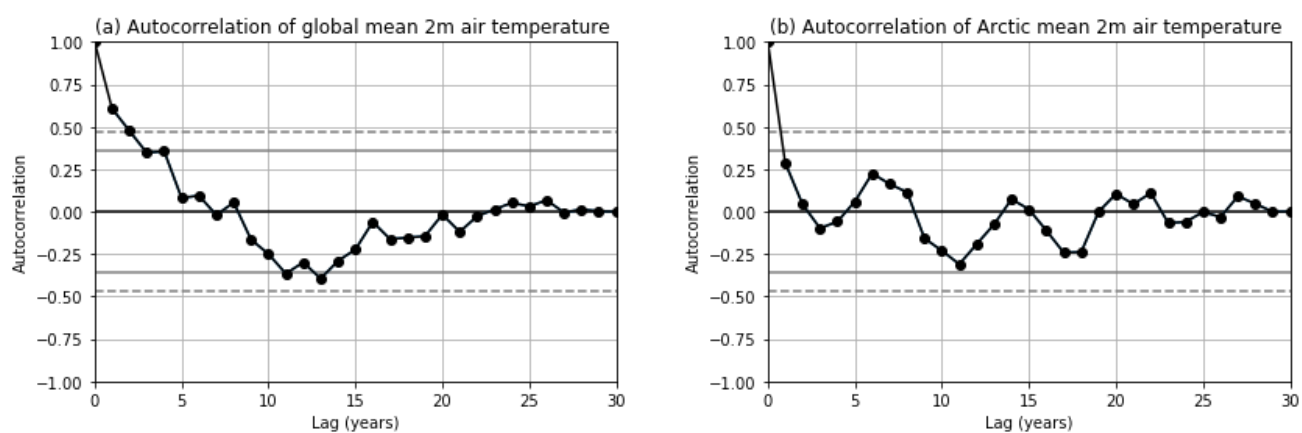


Figure S3: **Autocorrelation of 2m Air Temperature:** Autocorrelation of the area-weighted (a) global and (b) Arctic ($\geq 60^{\circ}\text{N}$) annual mean 2m air temperature, in the NLNL simulation.

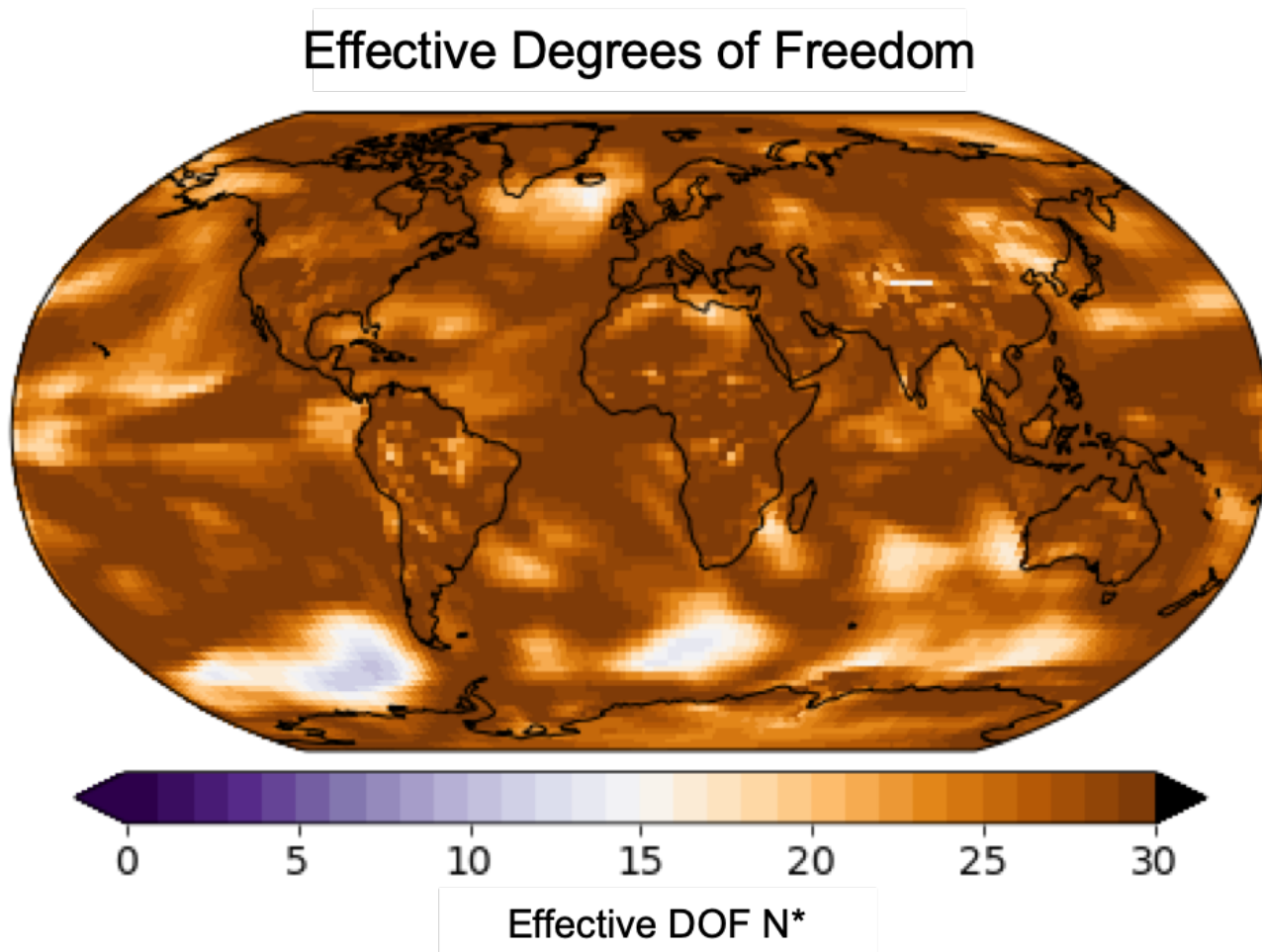


Figure S4: **Effective degrees of freedom N^*** : Calculated for a lag-1 (1-year) autocorrelation, for each gridcell, in the NLNL simulation.

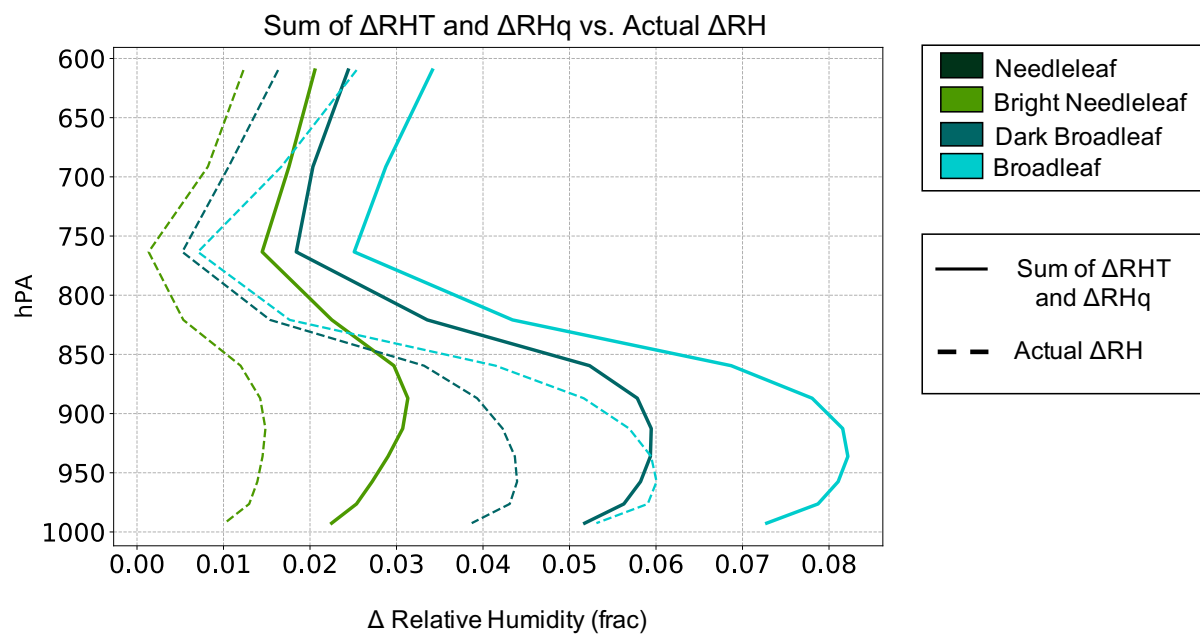


Figure S5: **Changes in RH:** Summer averages of the change in RH profile relative to the Needleleaf. Solid lines are the sum of the independent changes of RH due to temperature and specific humidity. Dashed lines are the changes in RH in simulations.

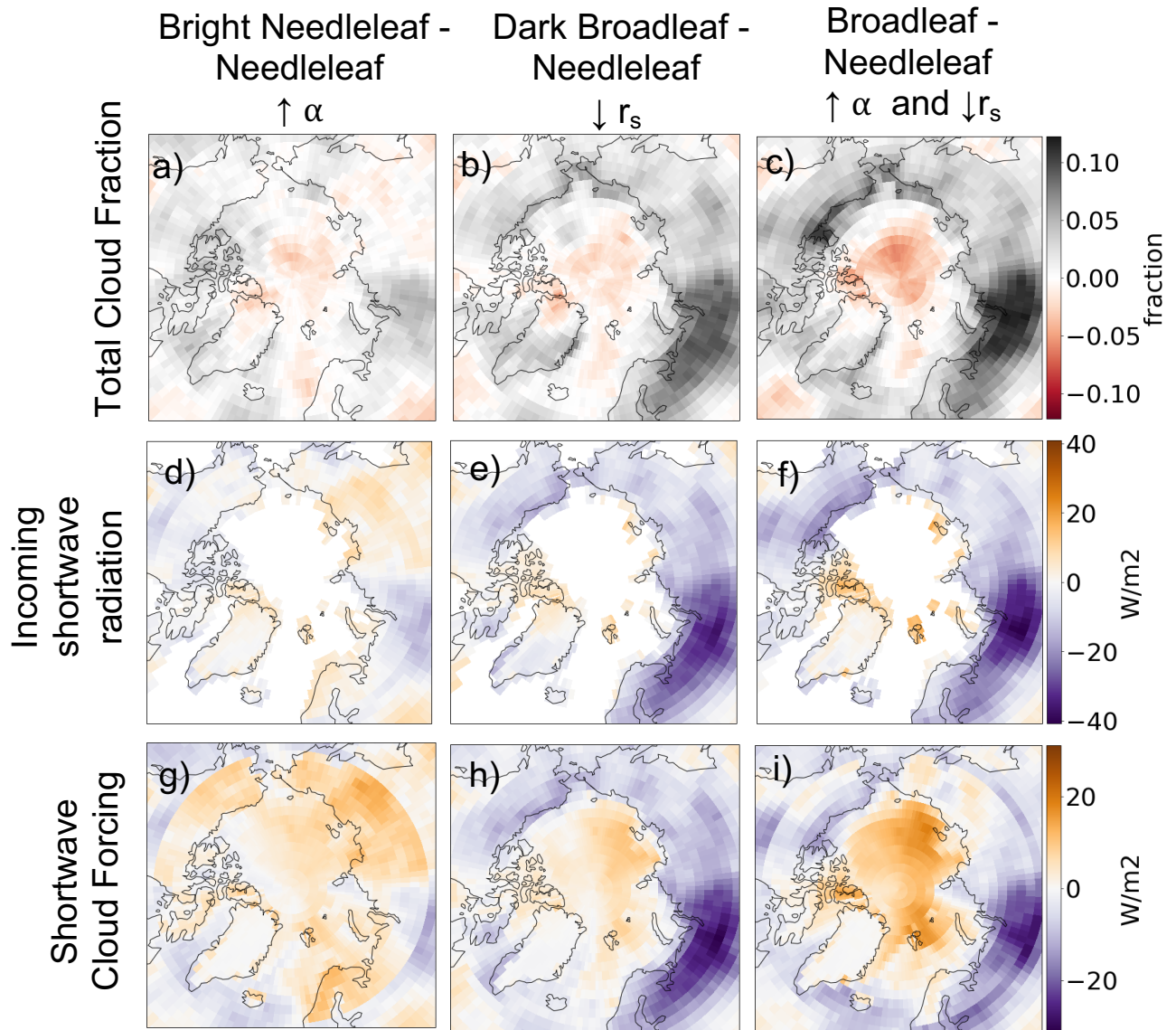


Figure S6: **Spatial patterns of change over the Arctic compared to Needleleaf simulation.** Changes in evaporative resistance (r_s) and albedo (α) for each case are relative to the Needleleaf case. First row (a-c) difference in total cloud fraction, second row (d-f) change in incoming shortwave radiation, third row (g-i) shortwave cloud forcing with negative values indicating greater shortwave cloud forcing (W/m²) at the surface. Surface temperature and shortwave absorbed are plotted only over land. Column 1 is the simulation where we increase albedo (α) alone (Bright Needleleaf - Needleleaf), Column 2 is where we decrease evaporative resistance (r_s) alone (Dark Broadleaf - Needleleaf), and column 3 is where we simultaneously increase albedo and decrease evaporative resistance (Broadleaf - Needleleaf).

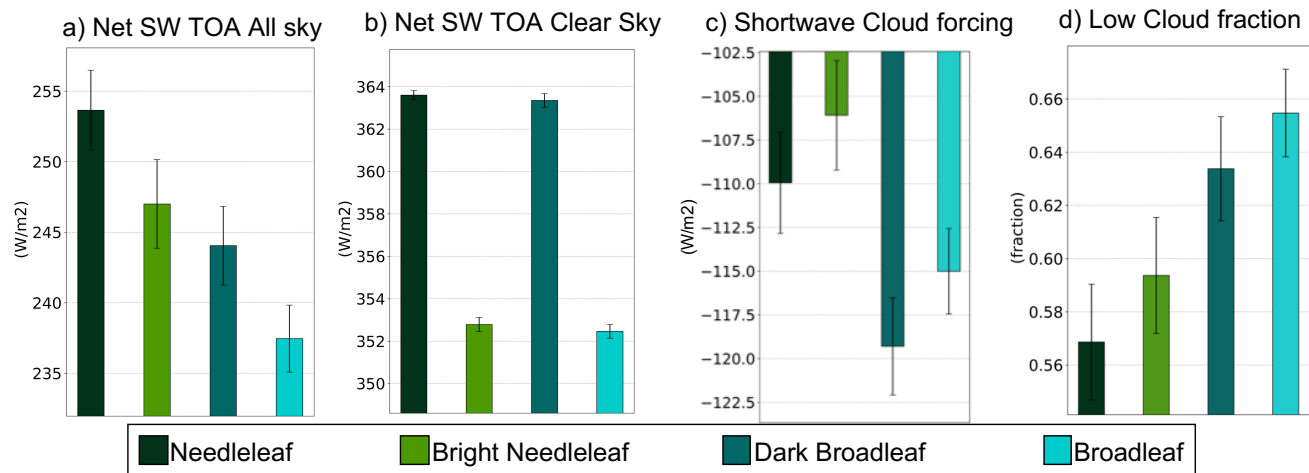


Figure S7: **Shortwave Cloud Forcing Components:** Summertime averages over non-glaciated land North of 60N for each of four different simulations (Needleleaf, Bright Needleleaf, Dark Broadleaf, Broadleaf) for a) net shortwave at the top of the atmosphere (TOA) for all sky conditions and positive values into the TOA (W/m²) b) net shortwave at the TOA for clear sky conditions and positive values into the TOA (W/m²), c) shortwave cloud forcing (W/m²) with greater negative values indicating greater cloud forcing (W/m²), d) low cloud fraction (fraction). The error bars represent one standard deviation of variability in time.

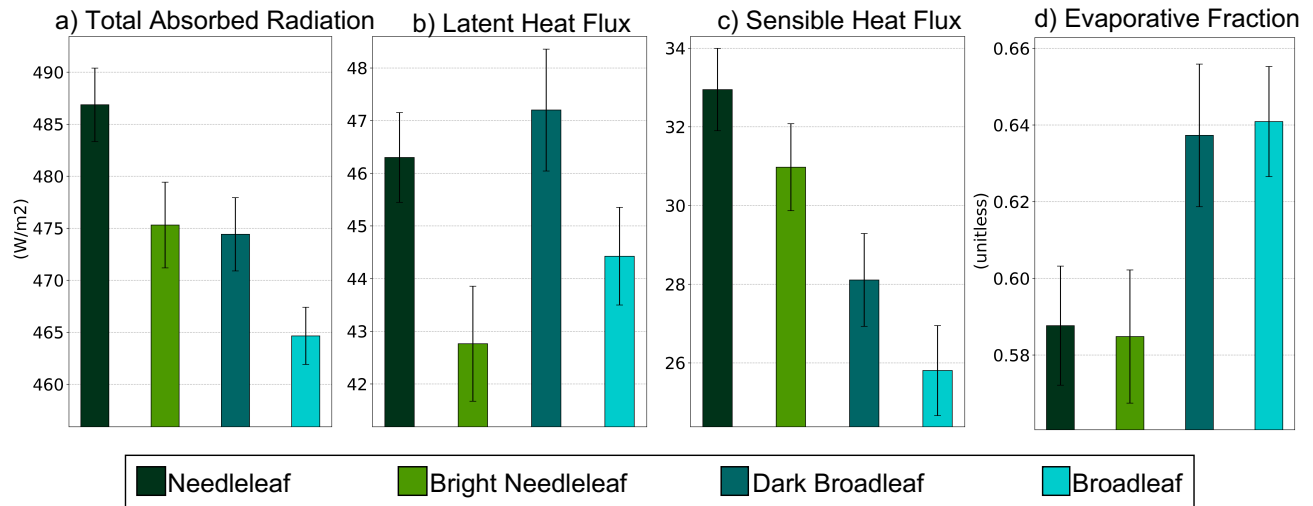


Figure S8: **Total absorbed radiation and turbulent fluxes.** Summertime averages over non-glaciated land North of 60°N for each of four different simulations (Needleleaf, Bright Needleleaf, Dark Broadleaf, Broadleaf) for a) total absorbed radiation at the surface with positive values into the surface (Wm^{-2}) b) latent heat flux (LH) with positive values indicating out of the surface (Wm^{-2}), c) Sensible Heat Flux (SH) with positive values indicating out of the surface (Wm^{-2}), d) Evaporative Fraction defined as $LH / (LH+SH)$. The error bars represent one standard deviation of variability in time.

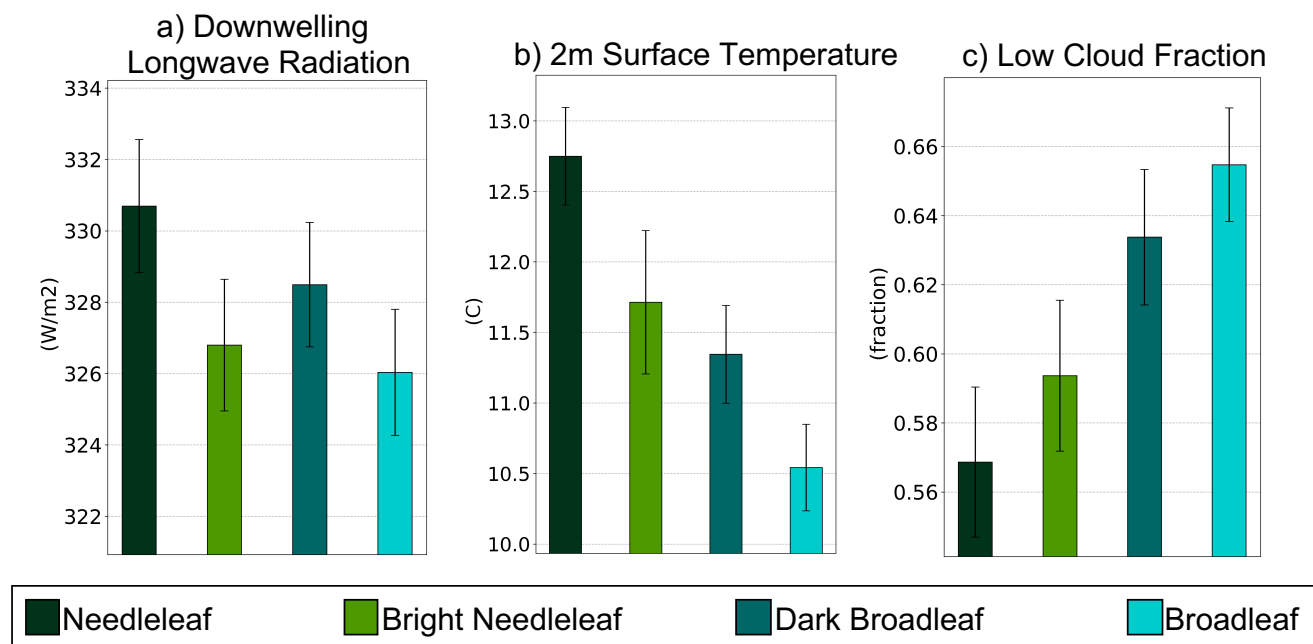


Figure S9: **Components of downwelling longwave radiation.** Summertime averages over non-glaciated land North of 60°N for each of four different simulations (Needleleaf, Bright Needleleaf, Dark Broadleaf, Broadleaf) for a) downwelling longwave radiation (Wm^{-2}) b) 2m surface temperature ($^{\circ}C$), c) low cloud fraction (unitless). The error bars represent one standard deviation of variability in time.

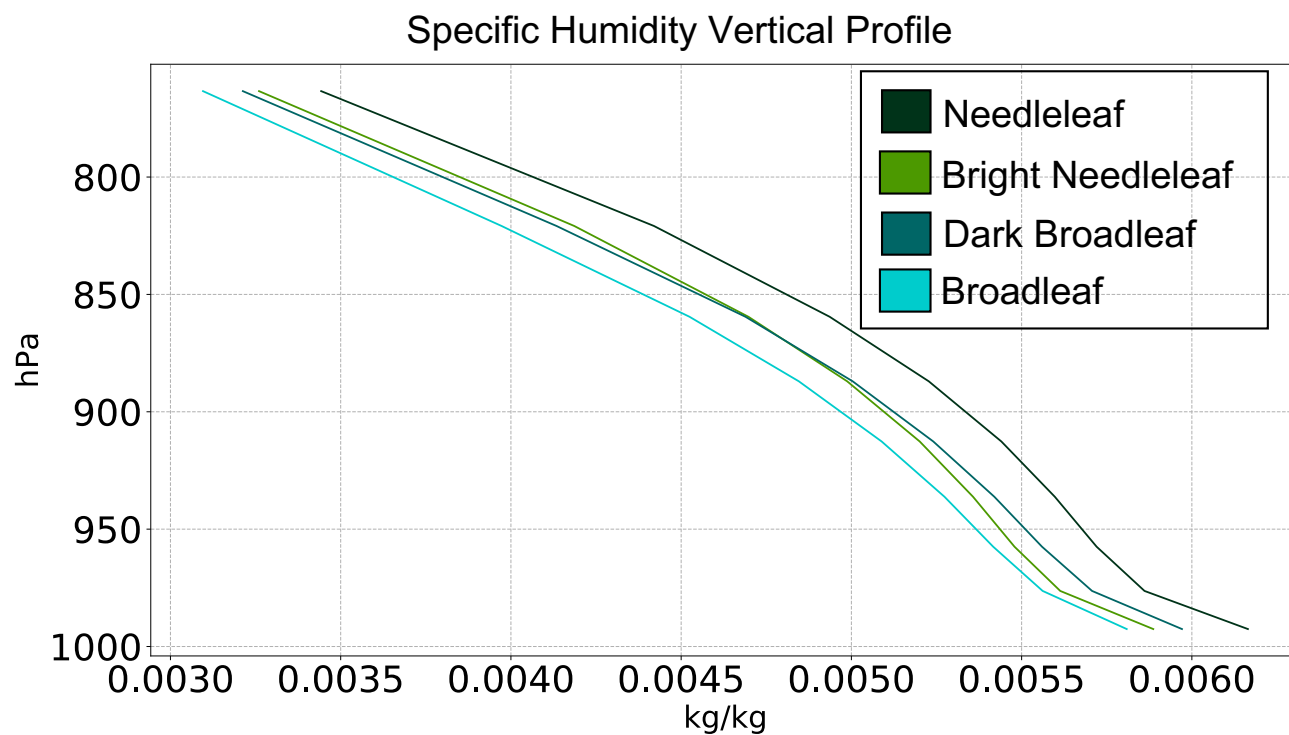


Figure S10: **Specific Humidity Vertical Profile.** Vertical profile of specific humidity with weighted averages over non-glaciated land North of 60°N for each of four different simulations (Needleleaf, Bright Needleleaf, Dark Broadleaf, Broadleaf)

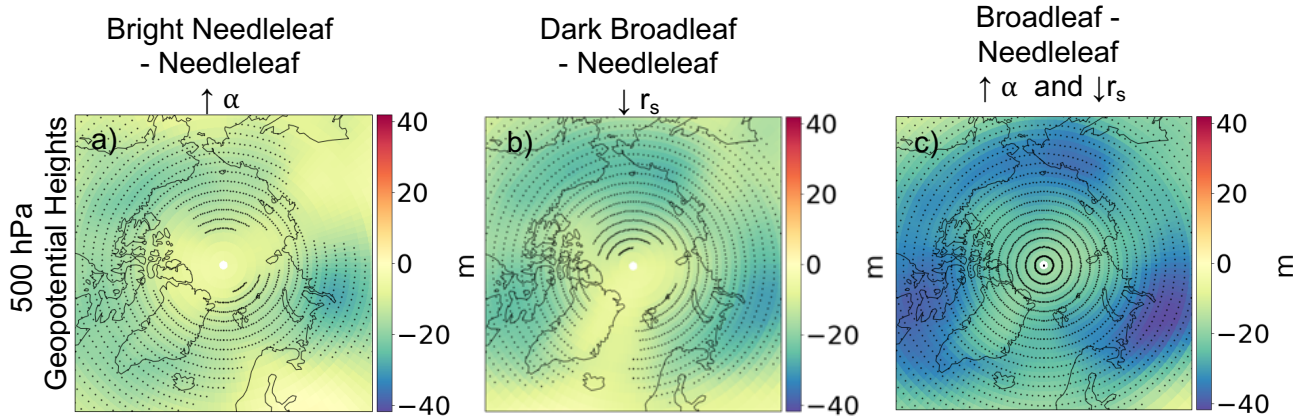


Figure S11: **Changes to the 500mb heights.** Each of the panels are changes to 500 hPa heights relative to the Needleleaf case. Panel a) is the simulation where we increase albedo (α) alone (Bright Needleleaf - Needleleaf), panel b) is where we decrease evaporative resistance (r_s) alone (Dark Broadleaf- Needleleaf), and panel c) is where we simultaneously increase albedo and decrease evaporative resistance (Broadleaf-Needleleaf). Stippling indicates significance.

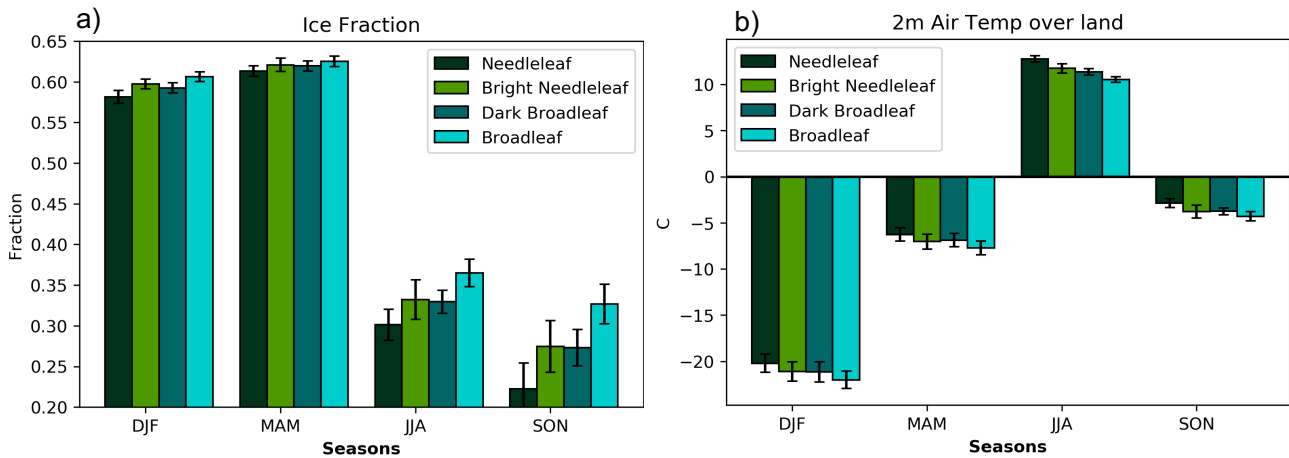


Figure S12: **Seasonal Sea Ice Fraction and 2m Air Temperature:** Panel a) shows the averages over non-land surfaces covered in sea ice North of 60N for each of the four different simulations (Needleleaf, Bright Needleleaf, Dark Broadleaf, Broadleaf) in each of the different seasons (DJF, MAM, JJA, SON). Panel b) shows the averages over non-glaciated land North of 60N for each of four different simulations (Needleleaf, Bright Needleleaf, Dark Broadleaf, Broadleaf) and for each of the different seasons (DJF, MAM, JJA, SON). The error bars represent one standard deviation of variability in time.